



AKADÉMIAI KIADÓ

Acta Microbiologica et  
Immunologica Hungarica

69 (2022) 4, 259–269

DOI:



[10.1556/030.2022.01881](https://doi.org/10.1556/030.2022.01881)

© 2022 Akadémiai Kiadó, Budapest

## RESEARCH ARTICLE



# Ginsenoside Rg1 modulates intestinal microbiota and supports re-generation of immune cells in dexamethasone-treated mice

SABIHA YOUSUF<sup>1†</sup>, HE LIU<sup>1†</sup>, ZHANG YINGSHU<sup>1</sup>,  
DANISH ZAHID<sup>1</sup>, HASSAN GHAYAS<sup>2</sup>, MING LI<sup>1\*</sup> ,  
YAN DING<sup>3\*</sup>  and WENZHE LI<sup>4\*</sup> 

<sup>1</sup> College of Basic Medical Sciences, Dalian Medical University, 9-Western Section, Lvshun South Road, Dalian, Liaoning, 116044, China

<sup>2</sup> Institute of Cancer Stem Cell, Dalian Medical University, Dalian, Liaoning, 116044, China

<sup>3</sup> School of Food Science and Technology, Dalian Polytechnic University, Dalian, Liaoning, 116034, China

<sup>4</sup> Guangdong Provincial Key Laboratory of Infectious Diseases and Molecular Immunopathology, Shantou University Medical College, Shantou, Guangdong, 515041, China

Received: September 17, 2022 • Accepted: October 17, 2022

Published online: November 11, 2022

## ABSTRACT

Ginsenoside Rg1 is one of the major ginsenosides found in roots of *Panax ginseng* and *Panax notoginseng*. Ginsenoside Rg1 is known to possess various biological activities including immunity enhancement activity. However, it is not clear whether the regulation of immune function by Rg1 is related to the intestinal microbiota. In the present study, the immuno-modulatory and gut microbiota-reshaping effects of ginsenoside Rg1 were evaluated. Ginsenoside Rg1 acts as an immune-enhancing agent to increase spleen index and the number of T, B and dendritic cells in dexamethasone (Dex)-treated mice. Ginsenoside Rg1 also increased the production of sIgA and regulated the expression of interleukin 2 (IL-2), IL-4, IL-10 and IFN- $\gamma$ . Meanwhile, Rg1 administration regulated the structure of intestinal microbiota. The relative abundance of mouse intestinal microbial groups, such as *Alistipes*, *Ruminococcaceae*, *Lachnospiraceae*, and *Roseburia* were increased by Rg1 administration, whereas a decrease in the potential pathogens like *Helicobacteraceae*, *Dubosiella*, *Mycoplasma*, *Alloprevotella*, *Allobaculum* was observed. Moreover, Rg1 metabolites of *Lachnospiraceae* bacterium enhanced the proliferation of CD4<sup>+</sup> T cells and T regulatory (Treg) cells. Ginsenoside Rg1 improved the inflammatory condition of the colonic tissue and repaired the destructed mucosal barrier. This study suggested that Rg1 strengthens immunity with regulating the homeostasis of intestinal microbiota in mice.

## KEYWORDS

Rg1, gut microbiota, immunity, lymphocytes, immunosuppression

## INTRODUCTION

The gastrointestinal tract is a barrier from harmful substances, this protection is provided by the association of epithelial and immune cells, alongside resident gut microbiota [1]. Gut microbiota plays important role in host-health status by adding in resistance to pathogens and influencing the immune system [2, 3]. Microbiota composition is affected by many factors such as dietary fiber [4], emulsifiers [5], and wholegrain intake [6]. Undesirable changes in gut microbiota structure can lead to diseases such as obesity [7], diabetes [8], colitis, and metabolic syndrome [5]. Microbiota can also influence the development of immune organs, as evident in germ-free mice studies by poor development of T and B cells and IgA producing plasma cells in lamina propria [9]. The microbiota structure is related to the

<sup>†</sup>Sabiha Yousuf and He Liu contributed equally to this work.

\*Corresponding authors.

E-mail: [liwenzhe@stu.edu.cn](mailto:liwenzhe@stu.edu.cn),  
[dingyan\\_515@hotmail.com](mailto:dingyan_515@hotmail.com),  
[vivianmarat@163.com](mailto:vivianmarat@163.com)



disease severity and dysfunction of immune responses in COVID-19 patients [10]. These studies indicated that homeostasis maintenance of microbiota is very important for keeping optimal host health.

Ginseng is an ancient herb that has been used for thousands of years in Asian countries. It has been used as a single herb or in a mixture of herbs in traditional Chinese medicine to treat diseases and promote health [11]. Pharmacological components of ginseng include ginsenosides, polyacetylenes and acidic polysaccharides [12]. Among them, ginsenosides are the most active components [13]. According to the steroidal structure and the number of hydroxyl groups/sugar moieties, ginsenosides are divided into protopanaxadiols (PPD), protopanaxatriols (PPT) oleanolic acids, and Ocotillol [14]. Ginsenoside Rg1 is the major PPT type ginsenoside, which is extracted from roots and rhizomes of the *Panax* genus (Family *Araliaceae*) [15]. Ginsenoside Rg1 and its metabolites possesses various biological activities such as neuroprotector, anti-depressant [16], anti-diabetic and hepatoprotective agent [17], anti-inflammatory effects [18] and hematopoietic function recovery [19]. Ginsenoside Rg1 promotes Th1 type differentiation of CD4<sup>+</sup> T cells, this action thus protected mice from the disseminated candidiasis [20]. Moreover, Rg1 induces the secretion of cytokines by human peripheral blood mononuclear cell (PBMC)-derived dendritic cells. It has been reported that the DSS-induced colitis is alleviated by Rg1 administration via regulation of T<sub>FH</sub>/Treg cells balance [21]. Several studies revealed the metabolism of Rg1 by gut microbiota of human and rat [22, 23], and its effect on the microbiota alterations in Alzheimer's disease model [24]. However, the function of Rg1 in enhancing immunity via microbiota composition remained unknown.

To assess the role of ginsenoside Rg1, we established a Dex-induced immunosuppressive mouse model and evaluated the effect of ginsenoside Rg1 on immune responses and change of gut microbiota composition. Our study suggested that ginsenoside Rg1 possesses immunomodulatory activity, and this effect is closely associated with its regulation of the homeostasis of intestinal microbiota.

## MATERIALS AND METHODS

### Isolation and purification of ginsenoside Rg1

*Panax notoginseng* was purchased from Jilin Province and authenticated by Jingbo Zhu professor through the Chinese Pharmacopoeia. Dried roots of *Panax ginseng* were ground to powder (1.3 kg) and dissolved in 3 L methyl alcohol (MeOH) and separated by a silica gel column to obtain 8 components. After thin layer chromatography (TLC) analysis, 8 samples were developed under the system of CHCl<sub>3</sub>: MeOH (7.5:2.5), and vanillin-concentrated sulfuric acid. The primary components were separated by Sephadex LH-20 and silica gel column chromatography, analyzed by TLC and high-performance liquid chromatography (HPLC), combined, and concentrated to obtain 11 components. Ginsenoside Rg1

(100 g) was obtained using super-30 column, recrystallization technology.

### HPLC analysis

AC Chrom S6000 spectrum liquid chromatography equipped with a binary solvent delivery system, autosampler, UV detector, Waters software, and C18 column (250 mm × 4.6 mm, 5 μm) was used for analysis during sample pretreatment. Mobile phases: acetonitrile (A) and deionized water (B). The elution gradient: 0–20 min, 20% A; 20–45 min, 20–46%A; 45–55 min, 46–55% A; 55–60 min, 55% A; 60–62 min, 55–90% A; 62–70 min, 90% A; 70–72 min, 90–20% A; and 72–80 min, 20% A. Column temperature: 30 °C, flow rate: 1.5 mL min<sup>-1</sup>, injection volume: 20 μL.

### Mice

Fifteen Kunming mice (18–22 g) were supplied from a specific pathogen-free (SPF) laboratory animal facility of Dalian Medical University, China. The mice were housed in a room under a light/dark cycle of 12/12 (h) and kept at 24 ± 1 °C with free access to food and water in the SPF laboratory environment. All protocols of this study were conducted according to the recommendations of animal work approved by the Ethics committee at the Dalian Medical University, China.

### Antibodies

FITC labeled anti-CD8 Ab (53-6.7), FITC labeled anti-NK cells (DX5) (11-5971-82), FITC labeled anti-CD11b Ab (M1/70), FITC labeled anti-Foxp3Ab (FJK-16s); PE labeled anti-CD3 Ab (145-2c11), PE-Cy5 labeled anti-CD19 Ab (1D3), PE-Cy5 labeled anti-CD4 Ab (L3T4); PE labeled anti-CD11c Ab (N418), PE labeled anti-F4/80 Ab (BM8), were obtained from e-Biosciences. APC labeled anti-CD4 Ab (H129.19) antibody was obtained from BD Pharmingen.

### Experimental grouping

Mice were divided randomly into three groups i.e., Control group (Control), Dexamethasone induced-immunosuppressed mice group (Dex), Rg1 intervention group (Dex + Rg1) (*n* = 5 per group). After completion of the acclimatization period (1 week), Dex and Dex + Rg1 group mice were subjected to an intraperitoneal injection of dexamethasone at a dosage of 20 mg kg<sup>-1</sup> for 7 days, while the Control group was injected with a phosphate-buffered solution (PBS). Afterward, Dex + Rg1 group mice were gavaged with soluble Rg1 solution (10 mg kg<sup>-1</sup>) for 21 days, the other two groups were gavaged with PBS. To evaluate the health status of the mice, body weight of mice was monitored daily. The stool samples for microbiota analysis were collected every 7 days from each group, including a 0-day sample.

### Histopathological examination

Mice in each group were sacrificed by cervical dislocation. After dissection, the colon tissues were collected, placed in



4% paraformaldehyde, and paraffin tissue sections were routinely prepared. Hematoxylin & eosin (H&E) staining was performed on paraffin sections and the histopathological morphology of the colon was observed under an optical microscope. Colon tissues were scored on a scale of 0–6 according to the degree of cell infiltration and tissue damage as described previously [25].

### Spleen index

The spleens of mice in different groups were collected and weighed aseptically to calculate the spleen index as follows: spleen index ( $\text{mg g}^{-1}$ ) = spleen mass (mg)/body mass (g). The splenic cells were obtained using frosted slides and passed through a 200-nylon mesh.

### Flow cytometric analysis (FACS)

Red blood cells of splenic cells were removed by incubation with RBCs lysis buffer (0.83%  $\text{NH}_4\text{Cl}$  in 0.17 M Tris-HCl) for 5 min at room temperature (RT). The cells were then incubated with an anti-CD16/CD32 (2.4G2) mAb to block the Fc $\gamma$  receptor at room temperature for 60 min and stained on ice for 60 min by different combinations of mAbs as shown in Figure legends. Flow cytometric analysis was done at FACS-Calibur (Becton Dickinson, Mountain View, CA), and the data were analyzed with the Cell Quest (Becton Dickinson) or Flowjo software (Treestar, SanCarlos, CA).

### Enzyme-linked immunosorbent assay (ELISA)

To extract the intestinal mucus the fat and connective tissue of the serosa were removed using forceps and scissors, and the intestine was transferred into a petri dish. The intestines of mice were cut open to remove the content and washed with PBS, homogenization was done in PBS solution containing 50 mM EDTA and 0.1  $\text{mg mL}^{-1}$  trypsin inhibitor. Homogenate was centrifuged at 10,000 rpm for 10 min and the supernatant was collected and stored at  $-80^\circ\text{C}$ . The sera were collected by centrifugation of blood at 5,000 rpm at  $4^\circ\text{C}$  for 15 min. The ELISA kit (Shanghai Langton Biological Technology Co., Ltd., China) was used to detect the contents of sIgA in serum and mucosa samples, according to the manufacturer's instructions. The absorbance was measured using a microplate reader (Thermo Scientific Multiskan) at 450 nm.

### Real-time PCR

Total RNA was extracted from splenic cells using RNAiso Plus reagent (TaKaRa, China). Real-time PCR analysis was performed using the StepOne Plus Real-Time PCR system. The thermal cycling conditions for real-time PCR were Hold for 30 s at  $95^\circ\text{C}$ , followed by 40 cycles of denaturation for 5 s at  $95^\circ\text{C}$  and annealing/extension for 30 s at  $60^\circ\text{C}$ . Primers used were as follows: 5'-CCT GAG CAG GAT GGA GAA TTA CA-3' and 5'-TCC AGA ACA TGC CGC AGAG-3' for IL-2; 5'-AGA TGG ATG TGA CAA ACG TCC TCA-3' and 5'-AAT ATG CGA AGC ACC TTG GAA GCC-3' for IL-4; 5'-GGT TGC CAA GCC TTA TCG GA-3' and 5'-ACC TGC

TCC ACT GCC TTG CT-3' for IL-10; 5'-AGA AGT AAG TGG AAG GCC CAG AAG-3' and 5'-AGG GAA ACT GGG AGA GGA GAA ATA T-3' for IFN- $\gamma$ ; 5'-AAA TGG TGA AGG TCG GTG TG-3' and 5'-TGA AGG GGT CGT TGA TGG-3' for GAPDH.

### Fecal DNA extraction and 16S rRNA sequencing

The microbial genomic DNA was extracted from stool samples of mice using the E.Z.N.A.<sup>®</sup> Stool DNA kit (Omega Bio-tek, Inc.) according to the manufacturer's instructions. The purity and concentration of isolated DNA were evaluated using Nanodrop 2000 spectrophotometer. The 16S rRNA gene V3-4 region of microbiota was amplified by PCR, using the sense primer (5'-ATT ACC GCG GCT GCT GG-3') and the anti-sense primer (5'-GGA CTA CHV GGG TWT CTA AT-3'). Library construction, qualification, sequencing, and analysis were done by the Illumina MiSeq platform (Personalbio Bioinformatics Technology Co., Ltd., Shanghai, China). The sequencing data were deposited in NCBI SRA under the accession number PRJNA692619.

### Cells and culture conditions

3–83 B (H-2K<sup>k</sup> and H-2K<sup>b</sup>) cells and Jurkat cells were purchased from the American type culture collection (ATCC). Cells were cultured in RPMI 1640 (Gibco, USA) supplemented with 2 mM glutamine, 50  $\mu\text{M}$  2-mercaptoethanol (2-ME) (Fluka, Buchs, Switzerland), 5% FCS, 100  $\text{U mL}^{-1}$  penicillin, 100  $\mu\text{g mL}^{-1}$  streptomycin (Sangon, China), and maintained in the incubator with 5%  $\text{CO}_2$  at  $37^\circ\text{C}$ .

### MTT assay

Cells were stimulated with Rg1 at concentration of 2  $\mu\text{g mL}^{-1}$ , and cell proliferation was measured using the 3-(4,5-dimethylthiazol-2-yl)-2,5 diphenyltetrazolium bromide (MTT, Sigma, Germany) at 0 h, 24 h, 48 h and 72 h. At each time interval cells were incubated with 10  $\text{mg mL}^{-1}$  MTT for 4 h at  $37^\circ\text{C}$ . After incubation, the media was removed and 200  $\mu\text{l}$  dimethyl sulfoxide (Sigma, Germany) was then added. The absorbance of each well was measure with a Benchmark microplate reader (Bio-Rad Laboratories, Hercules, CA, USA) at 490 nm.

### Stimulation of lymphocytes isolated from Peyer's patches (PPs) of mice

*Lachnospiraceae* bacterium (BAA-2278) was incubated in a BHI medium containing Rg1 for 24 h and centrifuged at 10,000 g for 15 min to obtain the supernatant containing metabolites of Rg1. The small intestines of mice were removed in a sterile environment and Peyer's patches (PPs) tissue was separated. The PPs tissue was ground and filtered through a 200-mesh sieve to obtain the PPs cell suspension. The PPs cells were stimulated with supernatant-containing metabolites of Rg1 (1/50 diluted) at  $37^\circ\text{C}$  for 4 h. BHI medium was used as control. After washing cells with PBS solution, the lymphocytes were blocked with anti-CD16/CD32 antibodies, and then incubated with PE-Cy5 labeled



anti-CD4, FITC labeled anti-Foxp3 and FITC labeled anti-CD3, PE-Cy5 labeled anti-CD19, and analyzed by flow cytometry.

### Statistical analysis

Statistical analysis was carried out using the ANOVA test by GraphPad Prism (version 6). A *P*-value of less than 0.05 was considered statistically significant. \**P* < 0.05, \*\**P* < 0.01, \*\*\**P* < 0.001.

## RESULTS

### Extraction and purification of ginsenoside Rg1

To assess the role of ginsenoside Rg1, we extracted Rg1 from dried roots of *P. ginseng*. Ginsenoside Rg1 (100 g) was further purified using super-30 column and recrystallization technology. NMR was used to determine the Rg1 structure. The <sup>1</sup>H-NMR (400 MHz, MeOD) δ: 5.13 (t, *J* = 6.9 Hz, 1H), 4.60 (dd, *J* = 21.3, 11.4 Hz, 1H), 4.37 (d, *J* = 7.8 Hz, 1H), 4.11 (td, *J* = 10.5, 3.0 Hz, 1H), 3.85 (d, *J* = 1.4 Hz, 1H), 3.83–3.80 (m, 1H), 3.78 (d, *J* = 2.0 Hz, 1H), 3.71 (dd, *J* = 10.4, 5.2 Hz, 1H), 3.67 (d, *J* = 5.1 Hz, 1H), 3.64 (dd, *J* = 5.0, 2.5 Hz, 1H), 3.40 (s, 1H), 3.37 (d, *J* = 4.2 Hz, 1H), 3.35 (d, *J* = 2.6 Hz, 1H), 3.33 (dt, *J* = 3.1, 1.7 Hz, 3H), 3.31 (s, 1H), 3.30 (s, 1H), 3.28 (d, *J* = 1.9 Hz, 1H), 3.24 (d, *J* = 3.2 Hz, 1H), 3.22 (s, 1H), 3.21 (d, *J* = 4.2 Hz, 1H), 3.15–3.11 (m, 1H), 3.10 (s, 1H), 3.08 (s, 1H), 2.41–2.23 (m, 1H), 2.18–2.00 (m, 3H), 2.03–1.91 (m, 1H), 1.90–1.80 (m, 2H), 1.80–1.72 (m, 2H), 1.70 (s, 4H), 1.68–1.57 (m, 7H), 1.57–1.39 (m, 2H), 1.36 (d, *J* = 7.2 Hz, 6H), 1.33–1.17 (m, 2H), 1.14 (d, *J* = 11.9 Hz, 5H), 1.02 (d, *J* = 3.8 Hz, 6H), 0.98 (s, 3H), 0.07–0.03 (m, 1H); <sup>13</sup>C-NMR (100 MHz, MeOD) δ: 16.48 (C-29), 17.22 (C-30), 17.45 (C-27), 17.86 (C-18), 17.88 (C-19), 23.2 (C-21), 25.7 (C-26), 27.56 (C-2), 28.07 (C-23), 28.76 (C-16), 31.74 (C-28), 32.33 (C-11), 32.63 (C-15), 33.71 (C-22), 39.69 (C-10), 39.8 (C-1), 40.63 (C-4), 41.44 (C-8), 45.15 (C-7), 50.41 (C-13), 50.69 (C-9), 50.82 (C-17), 50.9 (C-14), 61.45 (C-5), 63.13 (C-6''), 63.52 (C-6'), 69.85 (C-4'), 70.48 (C-4''), 71.98 (C-12), 74.16 (C-2''), 75.57 (C-2'), 77.82 (C-3''), 78.2 (C-3'), 78.92 (C-5'), 79.34 (C-6), 79.75 (C-3), 79.85 (C-5''), 80.24 (C-20), 96.9 (C-1''), 106.05 (C-1'), 123.84 (C-24), 131.07 (C-25). In HPLC analysis, we found that the purity of Rg1 extracts was more than 98% (Fig. 1A).

### Ginsenoside Rg1 improved the body weight and reduced mucosal barrier damage

Ginsenoside Rg1 is a protopanaxatriol (PPT) type ginsenoside, its structure is shown in Fig. 1B. In order to assess the immunomodulatory activities of Rg1 under immunosuppressed conditions, we established immunosuppressed mice model using Dex. Dex is a member of glucocorticoids, and glucocorticoids are known for their ability to cause immunosuppression [26]. Mice were divided randomly into three groups i.e., Control group (Control), Dex induced-immunosuppressed mice group (Dex), Rg1 intervention group

(Dex + Rg1) (Fig. 1C). Compared to the Control group (38.85 ± 3.81 g), the average body weights were significantly decreased in Dex group (34.9 ± 3.9 g), while body weight were recovered by Rg1 administration (39.4 ± 2.75 g) (Fig. 1D). Control group showed smooth and intact structure without inflammatory cells invasion and erosion of mucosal barrier in colon (Fig. 1E), while in the Dex group the colonic mucosal structure of mice was incomplete, the capillaries and lymphatic vessels of the lamina propria were dilated, the structure of the glands was distorted, and a large number of inflammatory cells were observed. Inflammatory cell infiltration and glandular structure were relieved in the Dex + Rg1 group, and the structural integrity of the mucosa was restored. The pathological scores of the Control group, the Dex group and Dex + Rg1 group were analyzed (*P* < 0.001) (Fig. 1F).

### Ginsenoside Rg1 improved immune functions of immunosuppressive mice

Upon necropsy, we observed that the spleen size in the Dex group mice was significantly reduced compared to the Control group and restored by Rg1 administration (*P* < 0.05) (Fig. 2A). Compared to the Control group, the spleen index was also significantly reduced in the Dex group and restored in the Dex + Rg1 group (*P* < 0.01) (Fig. 2B). Moreover, the number of splenic cells in the Dex group was significantly reduced compared with the Control group (*P* < 0.001) and increased after Rg1 administration (*P* < 0.01) (Fig. 2C). Next, we evaluated the effects of Rg1 on the generation of splenic cells. Flow cytometry analysis revealed that the proportion of CD3<sup>+</sup>, CD4<sup>+</sup> T, CD8<sup>+</sup> T cells, B cells (CD19<sup>+</sup>), and dendritic cells (CD11c<sup>+</sup>) were significantly decreased in the Dex group and recovered by Rg1 administration. However, no significant difference was found in the frequencies of NK (DX5<sup>+</sup>) and Foxp3 cells (Fig. 2D and E), indicated that Rg1 contributes to improve the population of immune lymphocytes.

The predominant immunoglobulin isotype in the mucosal immune system is the secretory IgA (sIgA) [27]. The sIgA is responsible to prevent the crossing of the epithelial layer by pathogens, commensal bacteria, and toxins, it also neutralizes intracellular pathogens, maintains homeostasis of commensals, and suppresses the pro-inflammatory responses [28]. To evaluate the effect of Rg1 on sIgA production, we detected the level of sIgA in the intestinal mucosa and serum by ELISA. As shown in Fig. 2F, the sIgA level was significantly reduced in the intestinal mucosa of Dex group mice, while it was increased in Dex + Rg1 group. In the serum, the level of sIgA was comparable between the Control group and Dex group (*P* < 0.05) (Fig. 2G). However, the sIgA was significantly increased by Rg1 administration (*P* < 0.01). Furthermore, the expression of genes required for immune responses was evaluated by real-time PCR. Expression of IL-2, IL-10 and IFN-γ were significantly down-regulated in Dex group, and these were restored in Dex + Rg1 group (Fig. 2H). Moreover, the expression of IL-4 was up-regulated in Dex group and restored to normal levels after Rg1 administration.



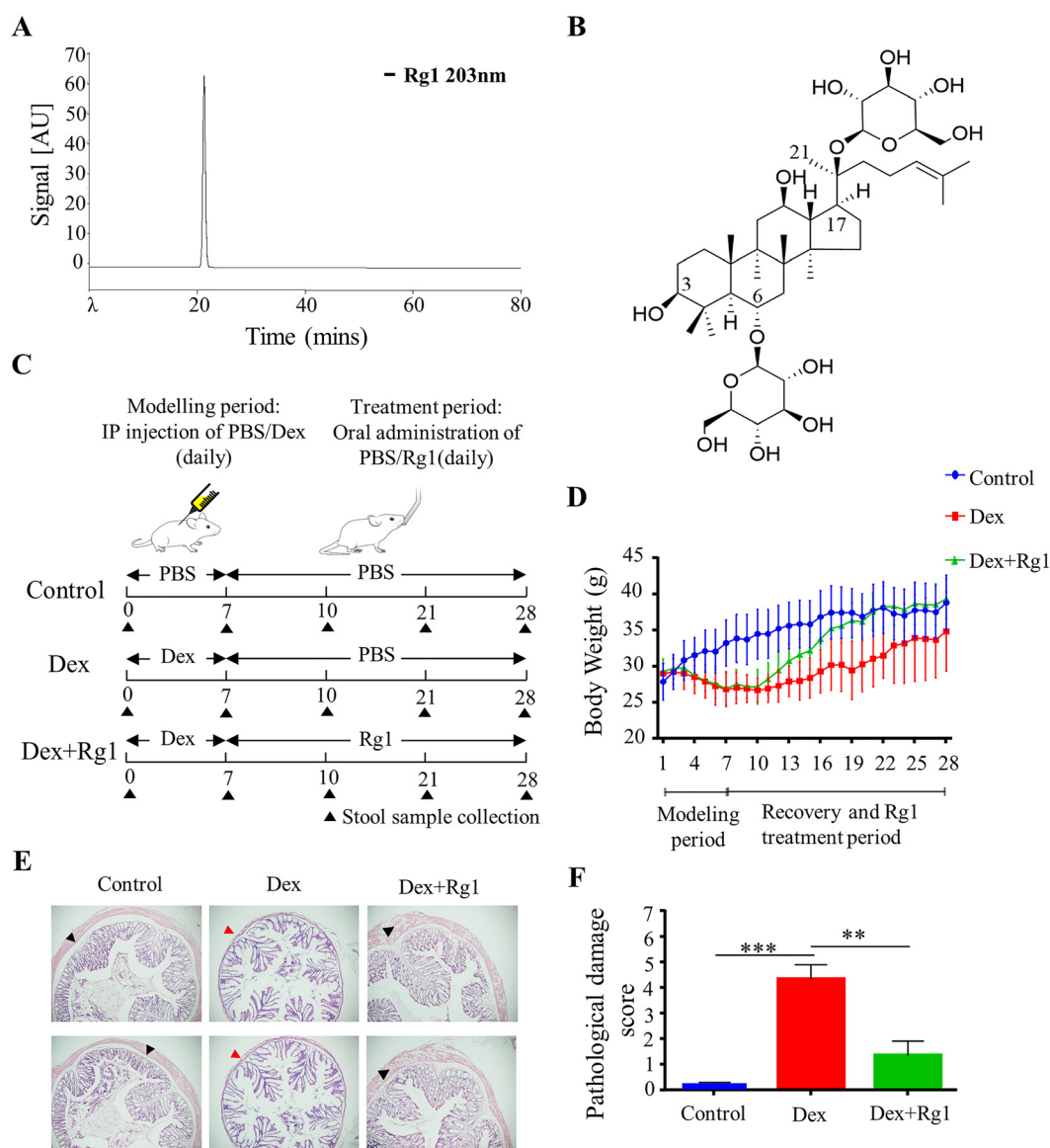


**Fig. 1.** Rg1 ameliorated Dex-induced weight loss and colonic tissue injury. **A.** HPLC analysis. A single peak of ginsenoside Rg1 purified is shown at 203 nm. **B.** Rg1 structure. **C.** Experimental design: Mice were divided into three groups; Control, Dex, and Dex + Rg1 group ( $n = 5$  for each group). For the initial 7 days, control group was injected with PBS intraperitoneally, while the other two groups were injected with Dex. For the next 3 weeks control and Dex group were gavaged with PBS while Dex + Rg1 was administered  $100 \text{ mg kg}^{-1}$  of Rg1. Fecal samples were collected on every 7 days. **D.** Changes of total weight in each group mice during the experiment. **E.** H&E staining of the colon tissue of mice in each group. Shown are damaged mucosal barrier (indicated with red arrow heads), intact mucosal barrier (black arrow heads). **F.** Histological scores of the colon histological damage in mice in each group (\*\* $P < 0.01$ , \*\*\* $P < 0.001$ )

### Ginsenoside Rg1 influenced the gut microbiota composition of immunosuppressive mice

To explore the effect of Rg1 on the structure of gut microbiota, 16S rRNA sequencing was performed. The microbial diversity of the samples could be reflected by the Shannon index. As shown in Fig. 3A, compared to the Control group, the microbial diversity decreased in the Dex group, while it was slightly increased in the Dex + Rg1 group.

The ordination analysis was further performed by NMDS. The clustering of Dex group is away from both Control and Dex + Rg1 group, revealing the differences among them, while

close clustering of Control and Dex + Rg1 group is evident of their similarities (Fig. 3B). The Unweighted pair group method with arithmetic mean (UPGMA) also showed obvious clustering separation between the Control group and Dex group, while the Dex + Rg1 group and Control group are in close clusters (Fig. 3C). The heat map was used to compare the genus level of the first 35 bacterial OTUs with relatively high abundance. On the level of phylum classification, control group and Dex + Rg1 group had higher similarities in Firmicutes and Tenericutes (Fig. 3D). Genus evolutionary tree showed *Helicobacteraceae*, *Dubosiella*, *Mycoplasma*, *Alloprevotella*, *Allobaculum* were enriched in the Dex group, but the

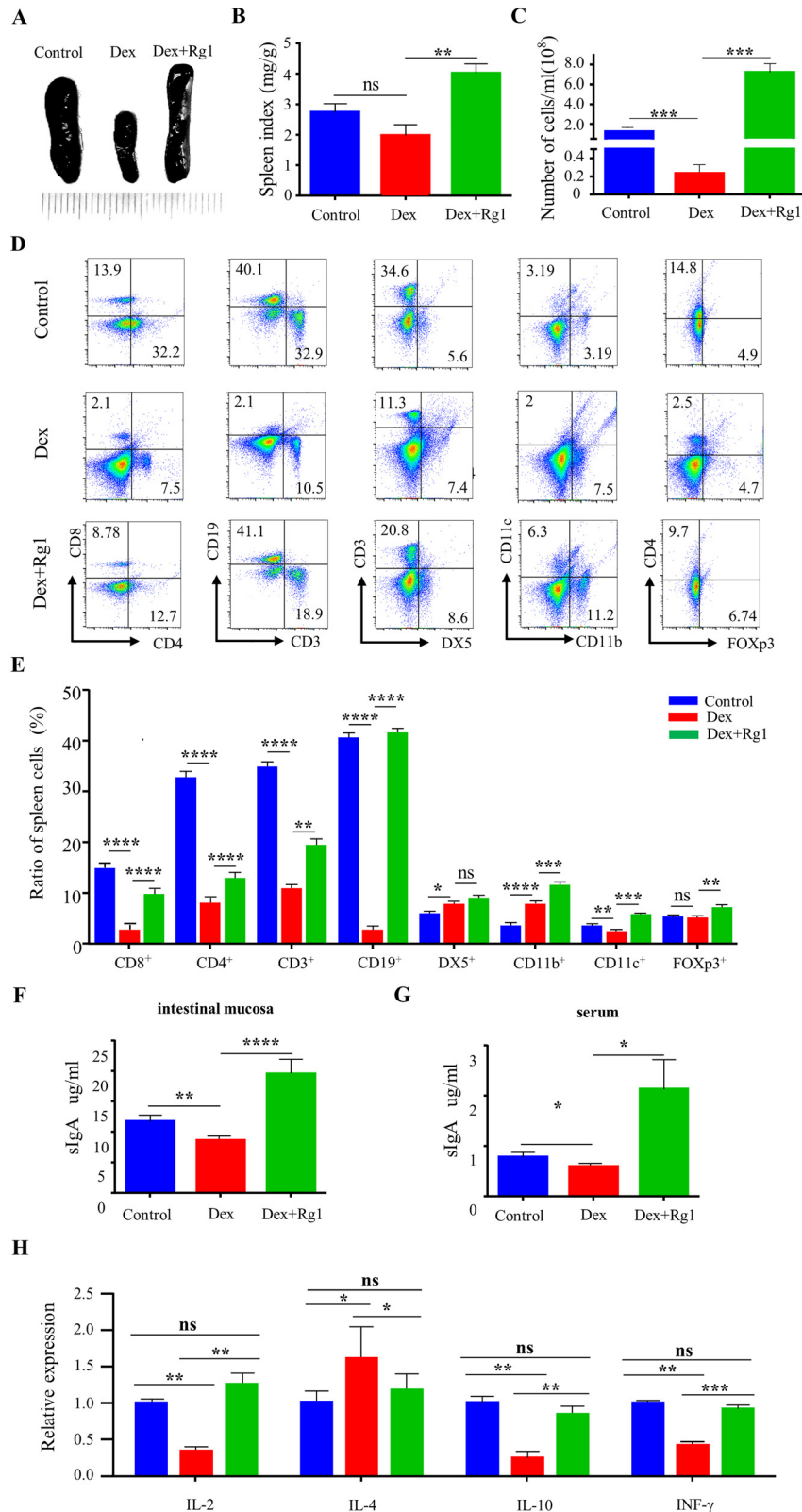


**Fig. 2.** Ginsenoside Rg1 improved immune functions of immunosuppressive mice. **A.** Comparison of spleen size between Control group, Dex group and Dex + Rg1 group. **B.** Spleen index of mice in each group. **C.** Total number of splenic cells in each group. **D.** Flow cytometry analysis. Population of splenic cells, such as CD8<sup>+</sup> T cells, CD4<sup>+</sup> T cells, CD19<sup>+</sup> B cells, CD3<sup>+</sup> T cells, NK cells (DX5<sup>+</sup>), dendritic cells (CD11c<sup>+</sup>), CD11b<sup>+</sup> cells, F4/80<sup>+</sup> cells, were analyzed. **E.** Population of lymphocytes in spleen of each group. **F.** ELISA analysis. The sIgA levels in small intestine were measured in Control group, Dex group and Dex + Rg1 group. **G.** The sIgA level in sera sample were measured by ELISA in each group. **H.** Real-time PCR analysis. Expression of IL-2, IL-10 and INF- $\gamma$  in Control group, Dex group and Dex + Rg1 group were detected. All data are representative of mean  $\pm$  SD from three independent experiments (\*\* $P < 0.001$ , \*\* $P < 0.01$ , \* $P < 0.05$ )



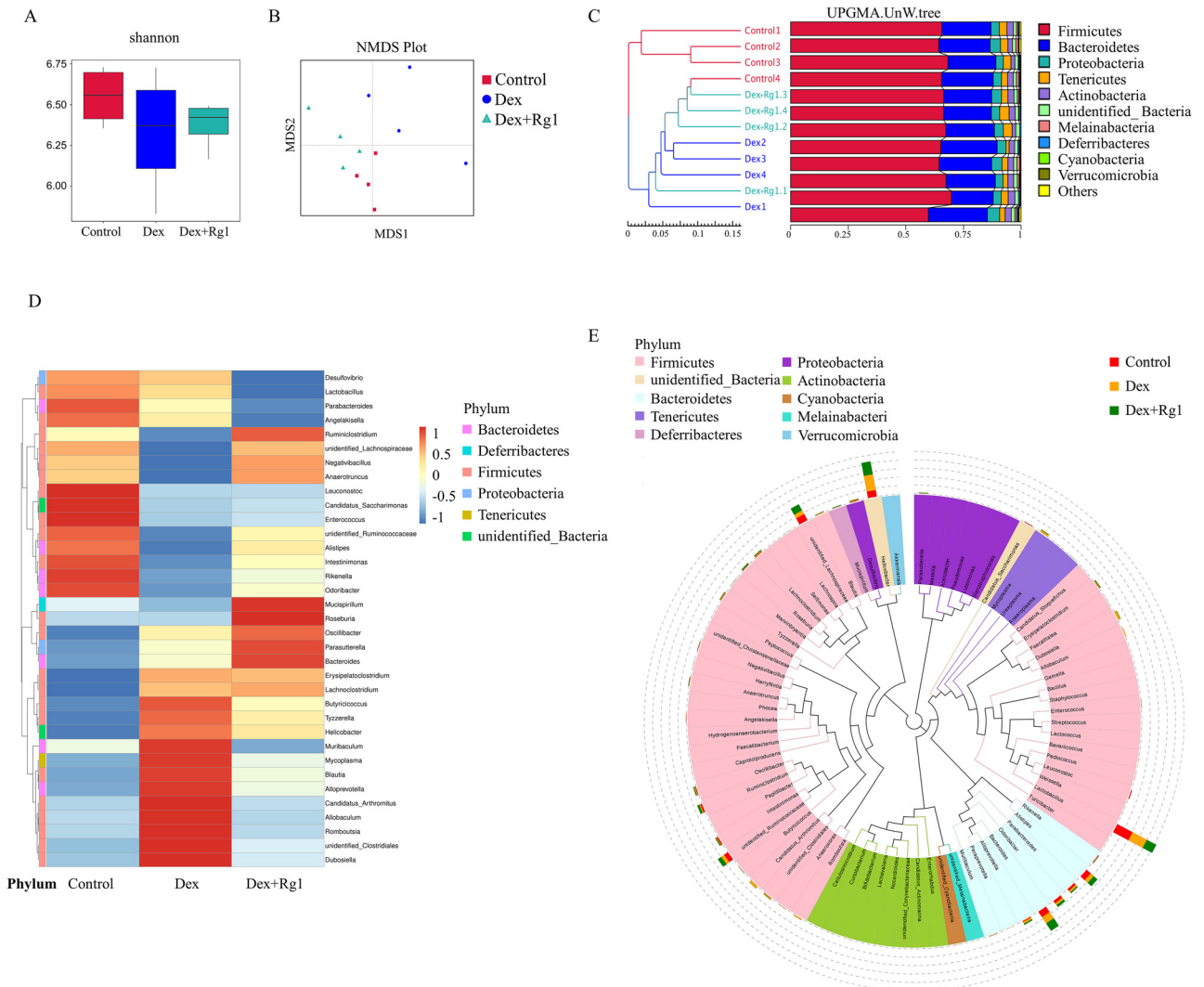


**Fig. 3.** Ginsenoside Rg1 influenced the gut microbiota composition of immunosuppressive mice. **A.** Comparison of Shannon's index of different groups. **B.** The nonmetric multidimensional scaling (NMDS) analysis shows the variation among samples within different groups. **C.** UPGMA tree of Unifrac distances of different groups. **D.** The heat map was used to compare the genus level of the first 35 bacterial OTUs with relatively high abundance. **E.** Genus evolutionary tree shows average abundance of microbial community in different groups at genus level

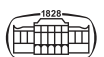
relative abundances of the above microbiota were decreased after Rg1 administration. Furthermore, the relative abundance of *Lachnospiraceae*, *Ruminococcaceae*, *Alistipes*, *Roseburia* were reduced in the Dex group, and returned to normal level in Dex + Rg1 group (Fig. 3E).

### Ginsenoside Rg1 did not promote the proliferation of B, T cell lines directly

As mentioned above, the numbers of splenic cells were significantly increased after Rg1 administration (Fig. 2C). To further clarify the effect of Rg1 on lymphocyte proliferation, we performed MTT assays using 3–83 B cells and Jurkat cells. The cell numbers were increased in 3–83 B cells after stimulation with Rg1 for 24 h, but no significant difference was observed at 48 and 72 h (Fig. 4A). Also, the cell growth was not changed with Rg1 treatment in Jurkat cells (Fig. 4B), suggesting that Rg1 did not affect cell proliferation directly.

### The Rg1 metabolites of *Lachnospiraceae* increased the generation of CD4<sup>+</sup> T cells and Treg cells

Since in vitro study did not show any effects of Rg1 on either 3–83 B cells or Jurkat cells, we speculated that the metabolites of intestinal microbiota in Rg1-administrated mice could affect their mucosal immune cells. To detect the effects of Rg1 metabolites produced by intestinal microbiota on the proliferation of B lymphocytes and T lymphocytes in the Peyer's patches of mice, we isolated total lymphocytes from the PPs and incubated them with Rg1 metabolites produced by *L. bacterium* (BAA-2278). As shown in Fig. 5A and B, the generation of CD4<sup>+</sup> T cells is significantly raised after treatment with *L. bacterium* (BAA-2278) Rg1 metabolites ( $P < 0.01$ ). Moreover, the generation of Treg (CD4<sup>+</sup>FOXP3<sup>+</sup>) cells is boosted after stimulation with Rg1 metabolites ( $P < 0.05$ ), while the proportion of B (CD19<sup>+</sup>) cells was not changed.



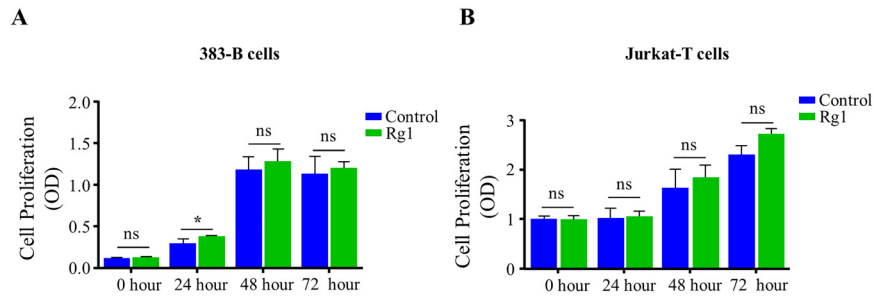


Fig. 4. Ginsenoside Rg1 did not promote the proliferation of B and T cell lines. A. MTT assay. The 3–83 B cells were treated with Rg1 for 0, 24, 48 and 72 h, and the cell proliferation was detected. B. MTT assay. The Jurkat cells were treated with Rg1 for 0, 24, 48 and 72 h, and the cell proliferation was detected (\* $P < 0.05$ )

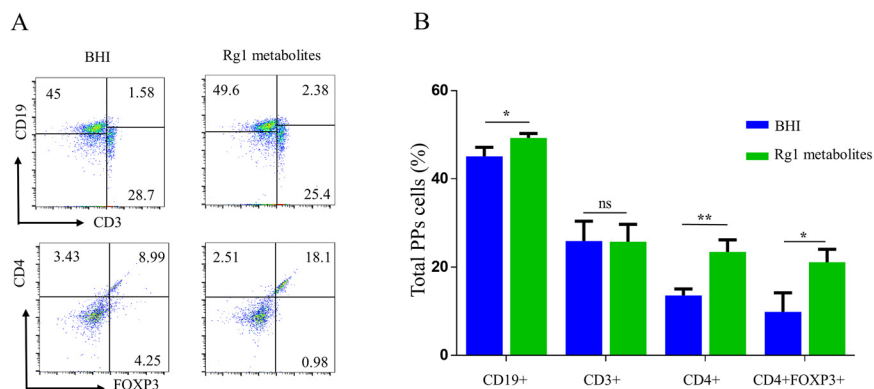


Fig. 5. Generation of CD4<sup>+</sup> T and Treg cells is increased by treatment of *Lachnospiraceae* Rg1 metabolites. A. FACS analysis. PPs cells were stimulated with Rg1 metabolites produced by *Lachnospiraceae bacterium* (BAA-2278). Brain-Heart Infusion (BHI) medium was used as control. The proportion of CD19<sup>+</sup> cells, CD3<sup>+</sup> cells, CD4<sup>+</sup> cells, and FOXP3<sup>+</sup> cells were then measured. B. Analysis of the proportion of PPs cells treated with Rg1 metabolites and BHI (control) (\*\* $P < 0.01$ , \* $P < 0.05$ )

## DISCUSSION

Ginsenoside Rg1, one of the main active components of ginseng, is a triterpenoid saponin compound. Researchers pay more attention to the role of ginsenoside Rg1 in anti-inflammatory properties, improve nonspecific immunity and hematopoietic functions in mouse models [18, 19, 29], however the interaction between ginsenoside and intestinal microbiota is still unknown. In the present study, we established a Dex-induced immunosuppressive mouse model, and found that ginsenoside Rg1 possesses immunomodulatory activity with regulating the homeostasis of intestinal microbiota.

Spleen modulates the immune responses as it consists of immune cells such as T and B lymphocytes, monocytes, and macrophages [30]. The spleen index reflects the status of host immunity [31]. The Dex causes immunosuppression by decreasing the number of lymphocytes and the weight loss of immune organs [32]. In the present study, the spleen index and the number of T cells, B cells, and dendritic cells were significantly reduced in the Dex group mice, and Rg1 administration improved the spleen index and the generation of the immune cells. CD4<sup>+</sup> T cells are subdivided into five subpopulations (Th1, Th2, Th17, Treg and T<sub>FH</sub>) based upon expression of specific lineage-defining transcription

factors, and cytokines production [33]. Cell-mediated inflammatory immunity is contributed by Th1 cells while Th2 cells elicit the humoral immune responses [34, 35]. Cytokines produced by the T cells directly or indirectly control the type of immune response, Th1 cells regulate the IL-2, IFN- $\gamma$ , and TNF- $\alpha$ , whereas Th2 cells modulate IL-4, IL-6, and IL-10 [36]. Expression of the IL-2, IL-10 and IFN- $\gamma$  was decreased in the Dex group, whereas the expression of IL-4 was increased, indicating the disbalance in the cytokine expression. Rg1 administration upregulates the expression of the IL-2, IL-10 and IFN- $\gamma$  and down-regulates the level of IL-4 to restore the dynamic balance of the Th1 and Th2 cells.

The gut microbiota is associated with many aspects of host physiology, and manipulation of the gut microbiota influences the host health [37], so we investigated the effect of Rg1 on intestinal microbiota in immunosuppressed mice. The 16S rDNA sequencing results show that the *Helicobacteraceae* family was increased in the microbiota of the Dex group. In the *Helicobacteraceae* family, mainly the *Helicobacter* species are associated with gastrointestinal disease in a broad range of hosts including both humans and animals [38]. *Helicobacter pylori* may be responsible for gastric cancer and gastroduodenal ulcer [39]. In the Dex group, the percentage of *Helicobacteraceae* was increased,



while it was reduced to some extent after Rg1 administration. Moreover, Rg1 administration released severe damage of mucosal barrier observed in the Dex group. It is conceivable that Rg1 protects the mucosal barrier from *Helicobacteraceae* infection. Rg1 administration also reduced the abundance of *Dubosiella* in immunosuppressed mice, whose increase is associated with conditions like colitis and obesity [40, 41]. *Alloprevotella* as a potential pathogen, enriched in the auditory meatus of otitis media patients [42], was also fertilized in the intestines of immunosuppressed mice but decreased under the intervention of Rg1. *Mycoplasma* was increased in the Dex group, while its relative abundance was declined to normal levels by Rg1 administration, *Mycoplasma* has been suspected for years to be involved in the etiology of Crohn's disease [43]. We also observed an increase in the relative abundance of the families of beneficial bacteria such as *Lachnospiraceae* and *Ruminococcaceae*. Daniel et al. [44] found that *Lachnospiraceae* is depleted in inflammatory bowel disease. Fujimoto et al. [45] found that *Faecalibacterium prausnitzii* (*Ruminococcaceae*) has decreased abundance in Crohn's disease. *Lachnospiraceae* and *Ruminococcaceae* both families are known to produce butyrate [46]. Anand et al. [47] found that butyrate is known to exert an anti-inflammatory response by stimulation of the Treg to increase the production of IL-10, which also increases the production of IgA by plasma cells to fight pathogenic bacteria in the gut lumen. Moreover, IgA production was stimulated in the presence of commensal bacteria of family *Lachnospiraceae* which expresses potent conserved B cell superantigens [48]. Coinciding with these findings our results of 16S rRNA sequencing showed the increase in *Lachnospiraceae* in the Dex + Rg1 group, and higher levels of the sIgA in intestinal mucous as well as serum. We assume that Rg1 is stimulating the production of sIgA via selective induction of GLT $\alpha$  expression in B cells [49] as well as an increase in the *Lachnospiraceae*. Previously, it is demonstrated that ginsenoside-Re is metabolized by human intestinal microbiota and transformed into Rh1 and F1 via Rg1 as intermediate and 20 (S)-protopanaxatriol is also detected as a minor component [23]. Bae et al. in their study showed that Rg1 is converted into 20 (S)-protopanaxatriol by gut microbiota of mice and humans via ginsenoside Rh1 and ginsenoside F1, and these metabolites of Rg1 exert anti-inflammatory effect by restoring Th17/Treg cells balance [18]. Similarly, our results depicted that direct stimulation of T cells with Rg1 did not lead to the proliferation of T cells, but when PPs cells were treated with *L. bacterium* Rg1 metabolites it stimulated CD4<sup>+</sup> T cells and Treg cells. Given that *Lachnospiraceae* are involved in the production of SCFAs (butyrate, propionate, and acetate), which are an important energy source for immune lymphocytes. Our research supports the hypothesis that Rg1 metabolites of *L. bacterium* promotes the generation of CD4<sup>+</sup> T cells and Treg cells. Further investigation of the Rg1 metabolites which are responsible for increase in generation of T cells by Rg1 is required.

In the present study, we revealed that Rg1 can strengthen immunity via manipulation of the Dex-induced intestinal

dysbiosis in mice and the improvement of immune cells and sIgA production, of which is closely associated with gut microbiota reshaping. Rg1 administration reduced the relative abundance of harmful bacteria like *Helicobacteriaceae* and increased the beneficial microbiota families *Lachnospiraceae* and *Ruminococcaceae*. Our study for the first time investigated the effects of ginsenoside Rg1 on the immune regulation via the intestinal microbiota reshaping, so as to provide theoretical and experimental basis for the popularization and application of ginsenosides.

*Conflict of interest:* The authors declare there no competing interests.

## ACKNOWLEDGMENT

This work was supported by the National Natural Science Foundation of China (32171279, 31870797, 31900920) and by the Liaoning Provincial Program for Top Discipline of Basic Medical Sciences.

## REFERENCES

- Cornick S, Tawiah A, Chadee K. Roles and regulation of the mucus barrier in the gut. *Tissue Barriers* 2015; 3(1–2): e982426.
- Chung H, Pamp SJ, Hill JA, Surana NK, Edelman SM, Troy EB, et al. Gut immune maturation depends on colonization with a host-specific microbiota. *Cell* 2012; 149(7): 1578–93.
- Arpaia N, Campbell C, Fan X, Dikiy S, van der Veeken J, deRoos P, et al. Metabolites produced by commensal bacteria promote peripheral regulatory T-cell generation. *Nature* 2013; 504(7480): 451–5.
- Desai MS, Seekatz AM, Koropatkin NM, Kamada N, Hickey CA, Wolter M, et al. A dietary fiber-deprived gut microbiota degrades the colonic mucus barrier and enhances pathogen susceptibility. *Cell* 2016; 167(5): 1339–53. e21.
- Chassaing B, Koren O, Goodrich JK, Poole AC, Srinivasan S, Ley RE, et al. Dietary emulsifiers impact the mouse gut microbiota promoting colitis and metabolic syndrome. *Nature* 2015; 519(7541): 92–6.
- Martínez I, Lattimer JM, Hubach KL, Case JA, Yang J, Weber CG, et al. Gut microbiome composition is linked to whole grain-induced immunological improvements. *ISME J* 2013; 7(2): 269–80.
- Dao MC, Clément K. Gut microbiota and obesity: concepts relevant to clinical care. *Eur J Intern Med* 2018; 48: 18–24.
- Qin J, Li Y, Cai Z, Li S, Zhu J, Zhang F, et al. A metagenome-wide association study of gut microbiota in type 2 diabetes. *Nature* 2012; 490(7418): 55–60.
- Kosiewicz MM, Zirnheld AL, Alard P. Gut microbiota, immunity, and disease: a complex relationship. *Front Microbiol* 2011; 2: 180.
- Yeoh YK, Zuo T, Lui GC-Y, Zhang F, Liu Q, Li AY, et al. Gut microbiota composition reflects disease severity and dysfunctional immune responses in patients with COVID-19. *Gut* 2021.
- Wan JY, Liu P, Wang HY, Qi LW, Wang CZ, Li P, et al. Biotransformation and metabolic profile of American ginseng



- saponins with human intestinal microflora by liquid chromatography quadrupole time-of-flight mass spectrometry. *J Chromatogr A* 2013; 1286: 83–92.
12. Kang S, Min H. Ginseng, the ‘immunity boost’: the effects of Panax ginseng on immune system. *J ginseng Res* 2012; 36(4): 354.
  13. Li J, Yang C, Zhang S, Liu S, Zhao L, Luo H, et al. Ginsenoside Rg1 inhibits inflammatory responses via modulation of the nuclear factor- $\kappa$ B pathway and inhibition of inflammasome activation in alcoholic hepatitis. *Int J Mol Med* 2018 Feb 1; 41(2): 899–907.
  14. Nag SA, Qin JJ, Wang W, Wang MH, Wang H, Zhang R. Ginsenosides as anticancer agents: in vitro and in vivo activities, structure-activity relationships, and molecular mechanisms of action. *Front Pharmacol* 2012; 3: 25.
  15. Wang JR, Yau LF, Gao WN, Liu Y, Yick PW, Liu L, et al. Quantitative comparison and metabolite profiling of saponins in different parts of the root of Panax notoginseng. *J Agric Food Chem* 2014; 62(36): 9024–34.
  16. Jiang B, Xiong Z, Yang J, Wang W, Wang Y, Hu ZL, et al. Anti-depressant-like effects of ginsenoside Rg1 are due to activation of the BDNF signalling pathway and neurogenesis in the hippocampus. *Br J Pharmacol* 2012; 166(6): 1872–87.
  17. Tian W, Chen L, Zhang L, Wang B, Li XB, Fan KR, et al. Effects of ginsenoside Rg1 on glucose metabolism and liver injury in streptozotocin-induced type 2 diabetic rats. *Genet Mol Res* 2017; 16(1).
  18. Lee SY, Jeong JJ, Eun SH, Kim DH. Anti-inflammatory effects of ginsenoside Rg1 and its metabolites ginsenoside Rh1 and 20(S)-protopanaxatriol in mice with TNBS-induced colitis. *Eur J Pharmacol* 2015; 762: 333–43.
  19. Xu SF, Yu LM, Fan ZH, Wu Q, Yuan Y, Wei Y, et al. Improvement of ginsenoside Rg1 on hematopoietic function in cyclophosphamide-induced myelosuppression mice. *Eur J Pharmacol* 2012; 695(1–3): 7–12.
  20. Lee JH, Han Y. Ginsenoside Rg1 helps mice resist to disseminated candidiasis by Th1 type differentiation of CD4+ T cell. *Int Immunopharmacol* 2006; 6(9): 1424–30.
  21. Jin J, Zhong Y, Long J, Wu T, Jiang Q, Wang H, et al. Ginsenoside Rg1 relieves experimental colitis by regulating balanced differentiation of Tfh/Treg cells. *Int Immunopharmacol* 2021; 100: 108133.
  22. He C, Feng R, Sun Y, Chu S, Chen J, Ma C, et al. Simultaneous quantification of ginsenoside Rg1 and its metabolites by HPLC-MS/MS: Rg1 excretion in rat bile, urine and feces. *Acta Pharm Sin B* 2016; 6(6): 593–9.
  23. Bae EA, Shin JE, Kim DH. Metabolism of ginsenoside Re by human intestinal microflora and its estrogenic effect. *Biol Pharm Bull* 2005; 28(10): 1903–8.
  24. Guo Y, Wang L, Lu J, Jiao J, Yang Y, Zhao H, et al. Ginsenoside Rg1 improves cognitive capability and affects the microbiota of large intestine of tree shrew model for Alzheimer’s disease. *Mol Med Rep* 2021; 23(4).
  25. Li Y, Liu M, Zhou J, Hou B, Su X, Liu Z, et al. Bacillus licheniformis Zhengchangsheng® attenuates DSS-induced colitis and modulates the gut microbiota in mice. *Benef Microbes* 2019; 10(5): 543–53.
  26. Xing K, Gu B, Zhang P, Wu X. Dexamethasone enhances programmed cell death 1 (PD-1) expression during T cell activation: an insight into the optimum application of glucocorticoids in anti-cancer therapy. *BMC Immunol* 2015; 16: 39.
  27. Leong KW, Ding JL. The unexplored roles of human serum IgA. *DNA Cell Biol* 2014; 33(12): 823–9.
  28. Corthésy B. Multi-faceted functions of secretory IgA at mucosal surfaces. *Front Immunol* 2013; 4: 185.
  29. Lee EJ, Ko E, Lee J, Rho S, Ko S, Shin MK, et al. Ginsenoside Rg1 enhances CD4(+) T-cell activities and modulates Th1/Th2 differentiation. *Int Immunopharmacol* 2004; 4(2): 235–44.
  30. Lori A, Perrotta M, Lembo G, Carnevale D. The spleen: a hub connecting nervous and immune systems in cardiovascular and metabolic diseases. *Int J Mol Sci* 2017; 18(6).
  31. Chen X, Nie W, Fan S, Zhang J, Wang Y, Lu J, et al. A polysaccharide from Sargassum fusiforme protects against immunosuppression in cyclophosphamide-treated mice. *Carbohydr Polym* 2012; 90(2): 1114–9.
  32. Li Y, Zheng B, Tian H, Xu X, Sun Y, Mei Q, et al. Yupingfeng Powder relieves the immune suppression induced by dexamethasone in mice. *J Ethnopharmacol* 2017; 200: 117–23.
  33. Geginat J, Paroni M, Maglie S, Alfen JS, Kastirr I, Gruarin P, et al. Plasticity of human CD4 T cell subsets. *Front Immunol* 2014; 5: 630.
  34. Mullen AC, High FA, Hutchins AS, Lee HW, Villarino AV, Livingston DM, et al. Role of T-bet in commitment of TH1 cells before IL-12-dependent selection. *Science* 2001; 292(5523): 1907–10.
  35. Das J, Chen CH, Yang L, Cohn L, Ray P, Ray A. A critical role for NF- $\kappa$ B in GATA3 expression and TH2 differentiation in allergic airway inflammation. *Nat Immunol* 2001; 2(1): 45–50.
  36. Constant SL, Bottomly K. Induction of Th1 and Th2 CD4+ T cell responses: the alternative approaches. *Annu Rev Immunol* 1997; 15: 297–322.
  37. Shepherd ES, DeLoache WC, Pruss KM, Whitaker WR, Sonnenburg JL. An exclusive metabolic niche enables strain engraftment in the gut microbiota. *Nature* 2018; 557(7705): 434–8.
  38. Solnick JV, Schauer DB. Emergence of diverse Helicobacter species in the pathogenesis of gastric and enterohepatic diseases. *Clin Microbiol Rev* 2001; 14(1): 59–97.
  39. Ernst PB, Gold BD. The disease spectrum of Helicobacter pylori: the immunopathogenesis of gastroduodenal ulcer and gastric cancer. *Annu Rev Microbiol* 2000; 54: 615–40.
  40. Sheng K, Zhang G, Sun M, He S, Kong X, Wang J, et al. Grape seed proanthocyanidin extract ameliorates dextran sulfate sodium-induced colitis through intestinal barrier improvement, oxidative stress reduction, and inflammatory cytokines and gut microbiota modulation. *Food Funct* 2020; 11(9): 7817–29.
  41. Bai YF, Wang SW, Wang XX, Weng YY, Fan XY, Sheng H, et al. The flavonoid-rich Quzhou Fructus Aurantii extract modulates gut microbiota and prevents obesity in high-fat diet-fed mice. *Nutr Diabetes* 2019; 9(1): 30.
  42. Mittal R, Sanchez-Luege SV, Wagner SM, Yan D, Liu XZ. Recent perspectives on gene-microbe interactions determining predisposition to otitis media. *Front Genet* 2019; 10: 1230.
  43. Roediger WE. Intestinal mycoplasma in Crohn’s disease. *Novartis Found Symp* 2004; 263: 85–93. discussion 93–8, 211–8.
  44. Frank DN, Amand ALS, Feldman RA, Boedeker EC, Harpaz N, Pace NR. Molecular-phylogenetic characterization of microbial community imbalances in human inflammatory bowel diseases. *Proc Natl Acad Sci* 2007; 104(34): 13780–5.
  45. Fujimoto T, Imaeda H, Takahashi K, Kasumi E, Bamba S, Fujiyama Y, et al. Decreased abundance of Faecalibacterium prausnitzii in the gut microbiota of Crohn’s disease. *J Gastroenterol Hepatol* 2013; 28(4): 613–19.



46. Duncan SH, Louis P, Flint HJ. Lactate-utilizing bacteria, isolated from human feces, that produce butyrate as a major fermentation product. *Appl Environ Microbiol* 2004; 70(10): 5810–7.
47. Anand S, Kaur H, Mande SS. Comparative in silico analysis of butyrate production pathways in gut commensals and pathogens. *Front Microbiol* 2016; 7: 1945.
48. Bunker JJ, Drees C, Watson AR, Plunkett CH, Nagler CR, Schneewind O, et al. B cell superantigens in the human intestinal microbiota. *Sci Transl Med* 2019; 11(507).
49. Shin BK, Kwon SW, Park JH. Chemical diversity of ginseng saponins from *Panax ginseng*. *J Ginseng Res* 2015; 39(4): 287–98.

